Pyrosequencing analysis yields comprehensive assessment of microbial communities in pilot-scale two-stage Membrane Biofilm Reactors

Aura Ontiveros-Valencia[1,2], Youneng Tang[1,3], He-Ping Zhao[1,4], David Friese[5], Ryan Overstreet[5], Jennifer Smith[6], Patrick Evans[6], Bruce E. Rittmann[1], Rosa Krajmalnik-Brown[1*].

[1]Biodesign Institute, Swette Center for Environmental Biotechnology, Arizona State University, 1001 South McAllister Ave. Tempe, AZ 85287-5701 USA

[2]School of Sustainability, Arizona State University

[3]University of Illinois at Urbana-Champaign, Urbana, IL 61801, USA (current affiliation)

[4] MOE Key Lab of Environmental Remediation and Ecosystem Health, College of Environmental and Resource Science, Zhejiang University, Hangzhou, China (current affiliation)

[5] APTwater, Inc., 100 W. Broadway, Suite 200, Long Beach, California 90802

[6] CDM-Smith, 14432 SE Eastgate Way, Bellevue, Washington 98007

*Corresponding author contact information: Telephone 1-480-727-7574, dr.rosy@asu.edu

Email: dr.rosy@asu.edu

Abstract

We studied the microbial community structure of pilot two-stage Membrane Biofilm Reactors (MBfRs) designed to reduce nitrate (NO_3^-) and perchlorate (ClO_4^-) in contaminated groundwater. The groundwater also contained oxygen (O_2) and sulfate (SO_4^{2-}), which became important electron sinks that affected the NO_3^- and ClO_4^- removal rates. Using pyrosequencing, we elucidated how important phylotypes of each "primary" microbial group –denitrifying bacteria (DB), perchlorate-reducing bacteria (PRB), and sulfate-reducing bacteria (SRB) -- responded to changes in electron-acceptor loading. UniFrac, principal coordinate analysis (PCoA), and diversity analyses documented that the microbial community of biofilms sampled when the MBfRs had a high acceptor loading were phylogenetically distant from and less diverse than the microbial community of biofilm samples with lower acceptor loadings. Diminished acceptor loading led to SO_4^{2-} reduction in the lag MBfR, and this allowed *Desulfovibrionales* (an SRB) and *Thiothrichales* (sulfur-oxidizers) to thrive through S cycling. Due to this cooperative relationship, they competed effectively with DB/PRB phylotypes such as *Xanthomonadales* and *Rhodobacterales*. Thus, pyrosequencing illustrated that, while DB, PRB, and SRB responded predictably to changes in acceptor loading, a decrease in total acceptor loading led to important shifts within the "primary" groups, the onset of other members (e.g. *Thiothrichales)*, and overall greater diversity.

Keywords: pilot MBfR, nitrate, perchlorate, sulfate, pyrosequencing (deep sequencing), community structure, community function.

Introduction

Nitrate (NO_3^-) is a prevalent water contaminant due to its heavy use in fertilizers and widespread presence in wastewater. NO_3^- can cause methemoglobinemia[1,2] in infants and spur eutrophication in water bodies. NO_3^- is regulated by the US EPA,[3] which established a maximum contaminant level (MCL) of 10 mg N/L for drinking water. Perchlorate (ClO_4^-) is an oxyanion with great chemical stability and is a constituent of rocket propellants, fireworks, and explosives. ClO_4^-, a normally recalcitrant contaminant found in waters of 35 US states and Puerto Rico,[4] can disrupt the thyroid after ingestion. Although ClO_4^- is not yet listed as a regulated chemical,[5] the USEPA is planning to issue an MCL.[6] NO_3^- and ClO_4^- often are found together at contaminated sites, because ammonium nitrate (NH_4NO_3), ammonium perchlorate (NH_4ClO_4), and potassium nitrate (KNO_3) are used together for the production of rocket fuel and explosives.[4]

Destruction of NO_3^- and ClO_4^- by microbial respiration has been well documented.[7-10] NO_3^- reduction can enhance or hinder ClO_4^- reduction[11-14] depending on the operating conditions of bioremediation approaches. Particularly, the inhibition of ClO_4^- reduction originates from the competition between denitrifying bacteria (DB) and perchlorate-reducing bacteria (PRB) for common resources, such as the electron donor,[15] space in biofilms,[15] and reductase enzymes.[16-18] However and regardless of possible complications, simultaneous microbial respiration of NO_3^- and ClO_4^- has been reported.[19-20] Furthermore, the need to manage the microbial communities in the system becomes even more pressing when in addition to NO_3^- and ClO_4^-, other electron acceptors such as sulfate (SO_4^{2-}) also are present in the water to be treated.

69 The presence of SO_4^{2-} in a NO_3^-- and ClO_4^- -contaminated groundwater was the
70 situation encountered during demonstration of a pilot two-stage Membrane Biofilm
71 Reactor (MBfR) system.[21] In the MBfR, hydrogen gas (H_2) diffuses through the walls of
72 hollow-fiber membranes and is used as electron donor by microorganisms that grow as a
73 biofilm on the membranes while utilizing oxidized compounds present in the water
74 flowing throw the reactor as electron acceptors.[22] Previous research with MBfR biofilms
75 pointed out competitive relationships between NO_3^- and ClO_4^- reductions for which a
76 NO_3^- loading above 0.6 g N/m^2 day at a fixed H_2-delivery capacity slowed ClO_4^-
77 reduction.[15]
78 Based on the desire to minimize competition between NO_3^- and ClO_4^-
79 reductions[11-18] when the groundwater to be remediated had a high NO_3^- : ClO_4^- ratio (~76
80 g N: 1 g ClO_4^-), Evans et al.[21] set up a two-stage pilot-scale MBfR. The lead MBfR
81 treated the raw groundwater and performed the bulk of denitrification. This lowered the
82 NO_3^- loading and the potential for NO_3^- reduction to compete with ClO_4^- reduction in the
83 lag MBfR, which received the effluent from the lead MBfR.[21] The strategy was mostly
84 successful, since most of the NO_3^- removal occurred in the lead MBfR; however, the two-
85 stage pilot MBfR could not consistently drive the ClO_4^- concentrations to below the
86 detection limit of 4 μg/L.[21]
87 In an initial effort to understand the pilot MBfR's performance, Zhao et al.[23]
88 assessed the microbial community structure of the pilot reactors using the quantitative
89 Polymerase Chain Reaction (qPCR) targeting characteristic reductases. DB (determined
90 by the nitrite reductases *nirK* and *nirS*) were the most abundant microbial group;
91 however, sulfate-reducing bacteria (SRB) (quantified by the dissimilatory sulfite

92 reductase *dsrA*) became dominant and may have outnumbered DB in the pilot MBfRs
93 when the NO_3^- + O_2 loading was low, below 0.3 g H_2/m^2 day.[23] PRB (quantified by the
94 perchlorate-reductase *pcrA*) were the smallest microbial fraction and were adversely
95 affected when SRB became important, a finding consistent with previous bench-scale
96 studies.[24]

97 In contrast to these pilot results, Ontiveros-Valencia et al.[25] was able to achieve
98 complete ClO_4^- reduction in a two-stage bench-scale MBfR, even though the ClO_4^-
99 concentration was unusually high (~4000 μg/L) and SO_4^{2-} was amply present (~55-60
100 mg/L). The success was attributed to an effective management of the microbial ecology
101 of the reactors so that SO_4^{2-} reduction was minimized, especially in the lag MBfR.
102 Ontiveros-Valencia et al.[25] suppressed SRB in the lag MBfR by re-oxygenating the
103 influent to the lag MBfR to increase the total-acceptor loading and by lowering the H_2
104 availability by either decreasing the H_2 pressure or by using a less-H_2 permeable
105 membrane. Neither strategy was followed with the pilot two-stage MBfR system: Re-
106 oxygenation of the effluent from the lead MBfRs was not possible with the pilot
107 configuration, and the pilot-MBfRs were mostly run with excess H_2 availability to
108 encourage ClO_4^- reduction.[21]

109 Added to the fact that treatment is more challenging when SO_4^{2-} is present in the
110 water to be treated, only limited information is available on the ecological interactions
111 between SRB and PRB. Waller[26] suggested that the microbial community structure of
112 consortia explored in her study was responsible for the decline in ClO_4^- reduction when
113 high SO_4^{2-} concentration was available. However, other studies reported no effect from

114 SO_4^{2-} on ClO_4^- microbial reduction[27-28]. Thus, more research addressing these critical
115 ecologic interactions is needed.
116 Although Zhao et al.[23] provided a broad view of the "primary" respiratory groups
117 (i.e., DB, PRB, and SRB) in the pilot MBfRs, we employ high-throughput
118 pyrosequencing to gain a deeper understanding of the microbial community structure,
119 including more insight into the phylotypes that constitute the primary respiratory groups
120 present when NO_3^-, ClO_4^-, and SO_4^{2-} are the electron acceptors and a view of other
121 members within the biofilm.
122 Our study addresses the ecological interactions among DB, PRB, SRB, and other
123 microbial groups that developed during bioremediation of groundwater polluted with
124 NO_3^- and ClO_4^- with SO_4^{2-} also present. In particular, we use UniFrac and principal
125 coordinate analysis (PCoA)[29,30] to demonstrate that distinctly different communities
126 developed in the biofilm when the acceptor-loading rate was decreased significantly.
127 Furthermore, we explore how decreased acceptor loading led to shifts within the primary
128 members and the development of important other members (e.g., heterotrophs and sulfur-
129 oxidizing bacteria) in the community. While Zhao et al.[23] used qPCR to provide an
130 analysis of community structure according to the primary respiratory groups, our findings
131 discriminate among conditions significantly altering the community structure, making the
132 biofilm more diverse and causing shifts within and outside the primary microbial groups.
133

Materials and Methods

MBfR configuration and performance

Detailed information about the pilot-MBfRs configuration is given by Evans et al.[21] and Zhao et al.[23] In brief, the two-stage MBfR was composed of two 500-gallon (1890-L) vessels containing 4 MBfR modules with membrane surface area of 144 m^2 per module. The manufacture and on-site configuration of the pilot-MBfR modules was done by APTwater and CDM-Smith. Figure 1a shows that the pilot-MBfR modules were cylindrical and made of woven fabric of polypropylene fibers, which formed sheets of fibers wrapped around a perforated acrylonitrile butadiene styrene (ABS) core. Each module contained ~140,000 polypropylene fibers (200μm OD, Teijin, LTD, Japan). H_2 gas diffused through the fiber sheet, and water passed through the perforations in the ABS core. The lead and lag MBfRs also were equipped with a set of side reactors for taking biofilm samples without disturbing the biofilm in the modules.[21,23] Figure 1b&c shows the side reactors with their connections for water and H_2.

The pilots were set up to treat a site historically used for munitions and explosives manufacture and surroundings agricultural fields. Hence, the oxidized contaminants in the groundwater were NO_3^- at 8-9 mg N/L and ClO_4^{2-} at 160-200 μg/L. The influent also contained O_2 at ~8 mg/L and SO_4^{2-} at ~22 mg/L. The lead and lag positions were switched every 3 days to make the biofilm development similar in both MBfRs and with the goal of minimizing the abundance of SRB in the lag MBfR.[21] The H_2 pressure and influent flow rate were adjusted according to the conditions in Table 1. The four conditions are representative periods of continuous operation of the pilot system. Adjustment of the influent flow rate led to a proportional change in the total electron-

157 acceptor surface loading: Conditions 3 and 4 had significantly lower total electron
158 acceptor loadings than did Conditions 1 and 2. The use of an excess H_2-delivery capacity
159 was done to ensure good NO_3^- removal in the lead MBfR and to achieve complete ClO_4^-
160 reduction in the lag MBfR.[21]

161 Samples were collected for off-site analysis at Test America (Irvine, CA), which
162 is certified by the California Environmental Laboratory Accreditation Program (ELAP).
163 The off-site assessment involved measurements for the lead and lag concentrations of
164 NO_3^- and SO_4^{2-} (US EPA method 300) and ClO_4^- (US EPA 314); they were performed
165 three, one, and three times per week, respectively. In addition, measurements for NO_3^-
166 and sulfide (as a surrogate for SO_4^{2-} reduction) were carried out three times per week on-
167 site using field kits (CHEMetrics, Virginia, USA).[21] O_2 and pH were measured by a hand
168 held probes.[21] The pH during operation was maintained between 7.4-7.8. The maximum
169 H_2 delivery capacity was calculated according to Tang et al. [31] and reported in Table 1.
170 Our work is complementary to the work reported by Zhao et al.[23], and both studies are
171 built on the field demonstration described by Evans et al.[21]

172 *Biofilm microbial ecology by pyrosequencing analysis*

173 Side reactors representing conditions 1, 2, 3, and 4 were taken after 60, 116, 221,
174 and 263 days of continuous operation, respectively, and were sent in ice containers to the
175 Swette Center for Environmental Biotechnology for microbial community analysis. The
176 samples arrived within 24 hours and were processed according to Zhao et al.[23] for DNA
177 extraction. DNA samples were stored at -80°C until shipping for 454 pyrosequencing.
178 DNA samples for 454 pyrosequencing were sent to the Molecular Research DNA lab
179 (Austin, Texas, USA), which performed amplicon pyrosequencing using a standard

Roche 454/GS-FLX Titanium.[32] The Bacteria domain was targeted by selecting the V6 and V7 regions of the 16S rRNA gene with primers 939F (5'-TTGACGGGGGCCCGCAC-3') and 1492R (5'TACCTTGTTACGACTT-3').[33] We processed the raw data using QIIME 1.7.0 suite[34] and removed sequences having fewer than 250 bps, homopolymers of more than 6 bps, primer mismatches, or an average quality score lower than 25. We picked the operational taxonomic unit (OTUs) using the Greengenes 16S rDNA database with *uclust* [35] based on ≥ 97% identity, removed OTUs that contain less than two sequences (singletons) from our analysis, and aligned the representative sequence of each OTU to the Greengenes Database using *PyNast*.[36,37] Potentially chimeric sequences were identified by using ChimeraSlayer,[38] and a python script in QIIME was employed to remove the chimeric sequences. We assigned taxonomy to OTUs with BLAST using the SILVA database[39] and constructed Newick-formatted phylogenetic trees using FasTree.[40]

For the purpose of eliminating heterogeneity related to having different numbers of sequences among the samples, we sub-sampled the OTU table by randomly selecting ten different times the lowest number of sequences (6800) found among the samples. We then generated PCoA plots and Unweighted Pair Group Method Arithmetic Mean (UPGMA) plots[30] using jack-knifed beta diversity.

We estimated the OTU richness by calculating Chao1,[41] which determines the asymptote on an accumulative curve, predicting how many OTUs would be present if a high number of sequences had been collected, and the phylogenetic relationships by using phylogenetic diversity (PD),[42] which estimates the cumulative branch lengths from random OTUs. To evaluate the microbial species diversity and evenness, we computed

203 the Shannon[43] and Simpson[44] indexes. A higher value for the Shannon index indicates
204 greater microbial diversity, while a value for the Simpson metric near one shows an even
205 distribution of bacterial groups within the sample. Sequence data sets are available at
206 NCBI/Sequence Read Archive (SRA) under study with accession number SRP038958.
207

Results and Discussion

Microbial community function

Table 2 synthesizes the performance of the pilot-scale reactors. The lead MBfRs were responsible for ~99% of the O_2 respiration, 70-90% denitrification, and a small loss of ClO_4^-.[21,23] In the lead MBfRs, the NO_3^- + O_2 flux was greater than ~ 0.34 g H_2/m^2-day[23] (Table 2), which completely suppressed SO_4^{2-} reduction and is consistent with the bench-scale results of Ontiveros-Valencia et al.[45] and modeling work by Tang et al.[46] Therefore, NO_3^- and SO_4^{2-} were the dominant electron acceptors entering the lag MBfR, and the total acceptor surface loading to the lag MBfR was much lower than for the lead MBfR (Table 1). Although the objective of reducing the flow rate and total acceptor loading for Conditions 3 and 4 was to enhance ClO_4^- removal in the lag MBfR, its major impact was to favor SO_4^{2-} reduction, an undesired outcome that led to lower ClO_4^- removal fluxes in the lag MBfR (Table 2).

Electron-acceptor loading affects microbial diversity and structure

Table S1 shows all the values for the diversity and evenness metrics for the four conditions. Overall, Chao1, Shannon, and PD values show that the microbial diversity of biofilm samples from Conditions 3 and 4, which had a low acceptor loading (Table 1), was greater than from Conditions 1 and 2, which had a higher acceptor loading. Consistent with the Chao1 results and based on the Simpson index, biofilm samples from Conditions 3 and 4 were more evenly distributed than those in Conditions 1 and 2.

Figure 2 shows the unweighted UniFrac analysis of the biofilm samples, which is based on the presence or absence of all the phylotypes within a sample. The biofilm

samples with high acceptor loading (Conditions 1 and 2) clearly formed a cluster (blue branch) distinct from the cluster of Conditions 3 and 4 (red branch). Thus, the large changes in acceptor loading between Conditions 2 and 3 led to very different microbial communities. Particularly for Conditions 1 and 2, the lead and lag biofilms were not significantly different due to the regular switching of positions.[21]

Figure 3 presents the unweighted PCoA plot, which reinforces the clustering found with the UniFrac analysis. The biofilm communities of Conditions 1 and 2 were close to each other along the PC1 vector, while those biofilm samples of Conditions 3 and 4 were distant. In an attempt to differentiate the driving force for the PC1 vector, we connect the removal fluxes for SO_4^{2-} and ClO_4^- (Table 2) with the community analysis by PCoA. Conditions 3 and 4 had importantly decreased average acceptor loadings (Table 1), and SO_4^{2-} reduction increased significantly (Table 2). The PC1 vector correlates with increased SO_4^{2-} reduction, particularly from Condition 2 to Condition 3. Hence, the microbial community structure was substantially modified when SO_4^{2-} reduction became a more important electron sink, a trend also noted by Ontiveros-Valencia et al.[33] Condition 2 was different from Conditions 1, 3, and 4 along the PC2 vector. This trend is most likely explained by the substantially higher ClO_4^- flux for Condition 2, which is illustrated in Table 2.

While the low electron acceptor loadings primarily shaped the microbial community, particularly by favoring SO_4^{2-} reduction, operation time also allowed biomass buildup[33,45] that may have contributed to structural changes in the biofilm communities. However, operational conditions, such as to the flow rate and hydraulic retention time (HRT), are directly connected to the electron acceptor loadings:

Decreased flow rate and the consequent higher HRT cause a lowered electron acceptor loading. Extra H_2 delivery capacity also can frame the community on its own; however, the excess capacity to deliver electron donor rates was similar across conditions, while the loading of electron acceptor was significantly modified.

Taxonomic breakdown and shifts in the microbial community structure

Figure 4 synthesizes the taxonomical break down at the order level of the most abundant phylotypes. Figure S1 also reports the ten most abundant phylotypes for all conditions at the genus level. Consistent with UniFrac and PCoA, the biofilm communities of the lead and lag MBfR were similar for each Condition. The brackets in the legend of Fig. 4 identify the known DB, PRB, SRB, and other types. The groupings show four important trends. First, ~86% of the taxonomic breakdown had microbial phylotypes most closely related to characterized DB and PRB for Condition 1, but these primary groups decreased for subsequent conditions, being only ~60% by Condition 4. Connecting this community trend to community function, DB and PRB phylotypes (reported by pyrosequencing in Figure 4) follow the same trend as the NO_3^-, O_2, and ClO_4^- fluxes (Table 2).

Second, the decrease of microbial phylotypes most closely related to DB and PRB was accompanied by significant increases in microbial phylotypes most closely related to SRB: from <1% in Condition 1 to ~13% in Condition 4. The SRB trend by pyrosequencing is similar to the SRB trend noted by Zhao et al.[23] using qPCR; however, the qPCR study found that SRB had become the largest primary group in Condition 4, followed by DB and PRB. It is possible that qPCR overestimated SRB, because some

277 DB harbor the *dsrA* gene.[47] Regardless of the method employed, the key trend is that
278 SRB became important with lower acceptor loading. As noted by Ontiveros-Valencia et
279 al.,[24] SRB become detrimental to PRB when they are able to occupy the most favorable
280 zones in the biofilm (near the H_2-delivering substratum).[46] Therefore, incomplete ClO_4^-
281 reduction in the lag MBfR can be at least partially attributed to increased competition
282 from SRB.

283 Third, lowered electron acceptor loadings leading to augmented SO_4^{2-} reduction
284 (Conditions 3 and 4) boosted the sulfur-oxidizing *Thiotrichales* and the SRB
285 *Desulfovibrionales.* This combination points towards a cooperative relationship based on
286 active S cycling in which *Thiotrichales* oxidizes H_2S produced by SRB while respiring
287 NO_3^- to ammonia (NH_4^+). Sulfide oxidation by *Thiotrichales* provided additional SO_4^{2-}
288 for SRBs, probably allowing SRB to grow to higher proportions than what would be
289 predicted from the one-time reduction of SO_4^{2-}. Figure S1 shows that closely related
290 *Thiothix* phylotypes, which belong to the *Thiotrichales* order, were abundant at
291 Conditions 3 and 4, and they might have imposed a risk for fouling the membranes due to
292 its filamentous growth.[49] *Thiothrix* can accumulate S granules in its interior from the
293 oxidation of H_2S and form rosettes, which are arrangements of filaments. [50-51] Staff
294 operating the pilot MBfRs reported observing filaments in some biofilms. Sulfide
295 oxidizers also were reported in MBfR biofilms by Zhao et al.,[52] who observed abundant
296 *Campylobacteriales* (sulfur-oxidizing bacteria), and by Ontiveros-Valencia et al.,[25] who
297 reported significant presence of *Ignavibacteriales* (green sulfur-oxidizing bacteria) and
298 *Thiobacteriales* (sulfur-oxidizing bacteria) when SO_4^{2-} reduction was favored in bench-
299 scale MBfRs. The differences in the phylotypes of the sulfur-oxidizers observed in the

bench- versus pilot-scale MBfRs probably can be attributed to the different inocula in each study. Despite the different inocula, the cooperative relationship between SRB and sulfur-oxidizing bacteria seems to be common once SO_4^{2-} reduction becomes important and seems to have accentuated an ecological advantage for SRB.

Besides sulfur-oxidizers, heterotrophic microorganisms such as *Bacteroidales* and *Flavobacteriales* increased in Conditions 3 and 4. The heterotrophs likely consumed soluble microbial products, whose rate of release increased with high rates of SO_4^{2-} reduction.[33,45] . Likewise, the relative abundance of "unclassified" bacteria and minor phylotypes (microbial groups at <1% abundance) (not shown in Figure 3) went from an average ~3% in Condition 1 to ~8% in Condition 4. The upswing of heterotrophs, unclassified bacteria, and minor phylotypes was the foundation for the increase in the microbial diversity with decreased acceptor loading (Table S1). The greater abundance of other groups and SRB certainly imposed more competition for space in the biofilm, forcing PRB to less favorable positions in the biofilm (zones more likely to detach).[24,46] Recently, Martin et al.[53] employed modeling to explain how increased detachment hindered MBfR performance. Thus, increasing diversity in the biofilm was correlated with poorer performance for ClO_4^- reduction.

Fourth, the DB and PRB groups showed important shifts with acceptor loading. In Conditions 1 and 2, *Rhodobacterales* were dominant; however, the most abundant DB and PRB phylotypes shifted to *Xanthomonadales* and *Rhodocyclales* in Conditions 3 and 4. In particular, closely related *Aquimonas* phylotypes, which belong to the *Xanthomonadales* order, were common to all biofilm samples, remaining in the biofilm regardless of competition (Fig. S1). In contrast, *Rhodobacterales* declined dramatically

323 in Conditions 3 and 4. Species *Rhodobacter capsulatus* and *Rhodobacter sphaeroides*
324 can reduce chlorate (ClO_3^-) to chlorite (ClO_2^-); however, no growth was associated with
325 this metabolism.[54]

326 Other substantial shifts in the phylotypes most closely related to DB and PRB
327 were observable. While the DB and PRB phylotype *Rhizobiales* remained relatively
328 constant across conditions, the phylotype *Hydrogenophilales* increased in Conditions 3
329 and 4. Lastly, phylotype *Burkholderiales* decreased abruptly while phylotype
330 *Pseudomonadales* decreased slightly. These substantial shifts in the DB and PRB
331 support that the biofilm communities were functionally redundant, which allowed
332 different phylotypes to gain or lose prominence as acceptor loading changed without
333 affecting denitrification performance.

334 In conclusion, pyrosequencing allowed us to comprehensively assess the
335 microbial community diversity and structure of pilot MBfRs. UniFrac, and PCoA helped
336 us understand the main drivers for the shifts in microbial structures. Biofilm
337 communities developed with low total acceptor loading were more diverse and
338 phylogenetic distant from communities with a higher acceptor loading. Primary members
339 (i.e., DB, PRB, and SRB) overall tracked the reduction of the electron acceptors, but
340 showed important shifts with acceptor loading. The DB/PRB phylotype *Rhodobacterales*
341 was significantly abundant at high acceptor loading; however, the phylotype
342 *Xanthomonadales* was overall the most dominant DB/PRB phylotype in all biofilm
343 samples. *Desulfovibrionales* and *Thiothrichales* appeared together at low acceptor
344 loadings and when SO_4^{2-} reduction was strong, suggesting S cycling that corresponded to
345 a slowing of the ClO_4^--reduction rate. Likewise, heterotrophic bacteria became more

346 important with lower acceptor loading. The abundance of SRB and sulfur-oxidizing
347 partners, as well as heterotrophs, likely accentuated competition for space and forced
348 PRB to less favorable positions in the biofilm. Thus, the increase in diversity with low
349 acceptor loading was due to the increases in SRB, sulfur-oxidizers, and heterotrophs, and
350 it correlated with poorer performance in terms of ClO_4^- reduction.
351
352 **Acknowledgements**
353 This research was funded by the Environmental Security Technology
354 Certification Program (ESTCP) by grant ER-200541. The authors express recognition to
355 the Consejo Nacional de Ciencia y Tecnologia (CONACYT) for providing a scholarship
356 to Aura Ontiveros-Valencia towards pursuing her graduate studies and conducting this
357 study.
358 **Supporting Information**
359 Alpha-diversity metrics and ten most abundant genera in biofilm samples across
360 the four conditions in the pilot system. This information is available free of charge via the
361 Internet at http://pubs.acs.org/

Table 1 Four Conditions identified H_2 availability (controlled by H_2 pressure) and electron-acceptor surface loadings (adjusted by influent flow rate) for lead and lag MBfRs

Condition	Flow rate m^3/d	Hydraulic Retention Time hours	H_2 pressure atm		NO_3^--N surface loading g H_2/m^2-d		O_2 surface loading g H_2/m^2-d		SO_4^{2-} surface loading g H_2/m^2-d		ClO_4^- surface loading g H_2/m^2-d		Total electron acceptor surface loading g H_2/m^2 day		Average electron acceptor loading g H_2/m^2 day
			lead	lag	lead	lag	lead	lag	lead	lag	lead	lag	lead	lag	
1	65	0.7	2.2	1.8	0.41	0.13	0.15	0.002	0.22	0.22	0.002	0.002	0.78	0.36	0.6
2	98	0.5	2.8	2.3	0.66	0.17	0.23	0.006	0.33	0.33	0.003	0.002	1.22	0.51	0.9
3	44	1.0	2.2	2	0.37	0.03	0.10	0.002	0.18	0.18	0.002	0.0004	0.65	0.22	0.4
4	33	1.4	2.1	1.6	0.23	0.02	0.08	0.0004	0.11	0.11	0.001	0.0002	0.41	0.13	0.3

We calculated the electron acceptor loading rates according to:

$$Loading = \frac{Q \times (S^{\circ})}{A} \qquad (eq. 1)$$

where Q = volumetric flow rate (L/day), A = membrane surface area (m^2), and S° is the influent concentration (g/L) for an electron acceptor. Each electron acceptor loading value was normalized to g H_2/m^2 day based on stoichiometric relationships described elsewhere.[15-23-25] Total electron-acceptor loading was calculated as the sum of the loadings for O_2, NO_3^-, ClO_4^-, and SO_4^{2-}. The average electron acceptor loading was calculated from the lead and lag total electron acceptor loadings at each condition. The lead and lag positions were switched every three days; therefore, an average estimate of the acceptor loading is valuable. The HRT was the same for each reactor regardless of the position.

Table 2 Electron acceptor and donor fluxes for lead and lag MBfRs for the four conditions tested over time

Condition	**Nitrate** $g\ H_2/m^2\ day$		**Oxygen flux** $g\ H_2/m^2\ day$		**Sulfate flux** $g\ H_2/m^2\ day$		**Perchlorate flux** $g\ H_2/m^2\ day$		**Total H_2 experimental flux** $g\ H_2/m^2\ day$		**Maximum H_2 flux** $g\ H_2/m^2\ day$		**Oversupply of H_2** $g\ H_2/m^2\ day$	
	Lead	Lag	Lead	Lag	Lead	Lag	Lead	Lag	Lead	Lag	Lead	Lag	Lead	Lag
1	0.28	0.13	0.15	0.002	0	0.0006	0	0.0008	0.43	0.13	0.57	0.46	0.14	0.3
2	0.49	0.17	0.21	0.004	0	0.001	0.001	0.0018	0.7	0.2	0.72	0.59	0.02	0.4
3	0.24	0.03	0.09	0.002	0	0.0026	0.0007	0.00038	0.33	0.03	0.57	0.51	0.24	0.48
4	0.2	0.02	0.07	0.0004	0	0.003	0.0007	0.00019	0.27	0.02	0.53	0.41	0.26	0.39

The electron acceptor fluxes were reported elsewhere.[23] The maximum H_2 flux was calculated as Tang et al.[31] and the oversupply of H_2 corresponded to the maximum H_2 flux minus the total H_2 experimental flux.

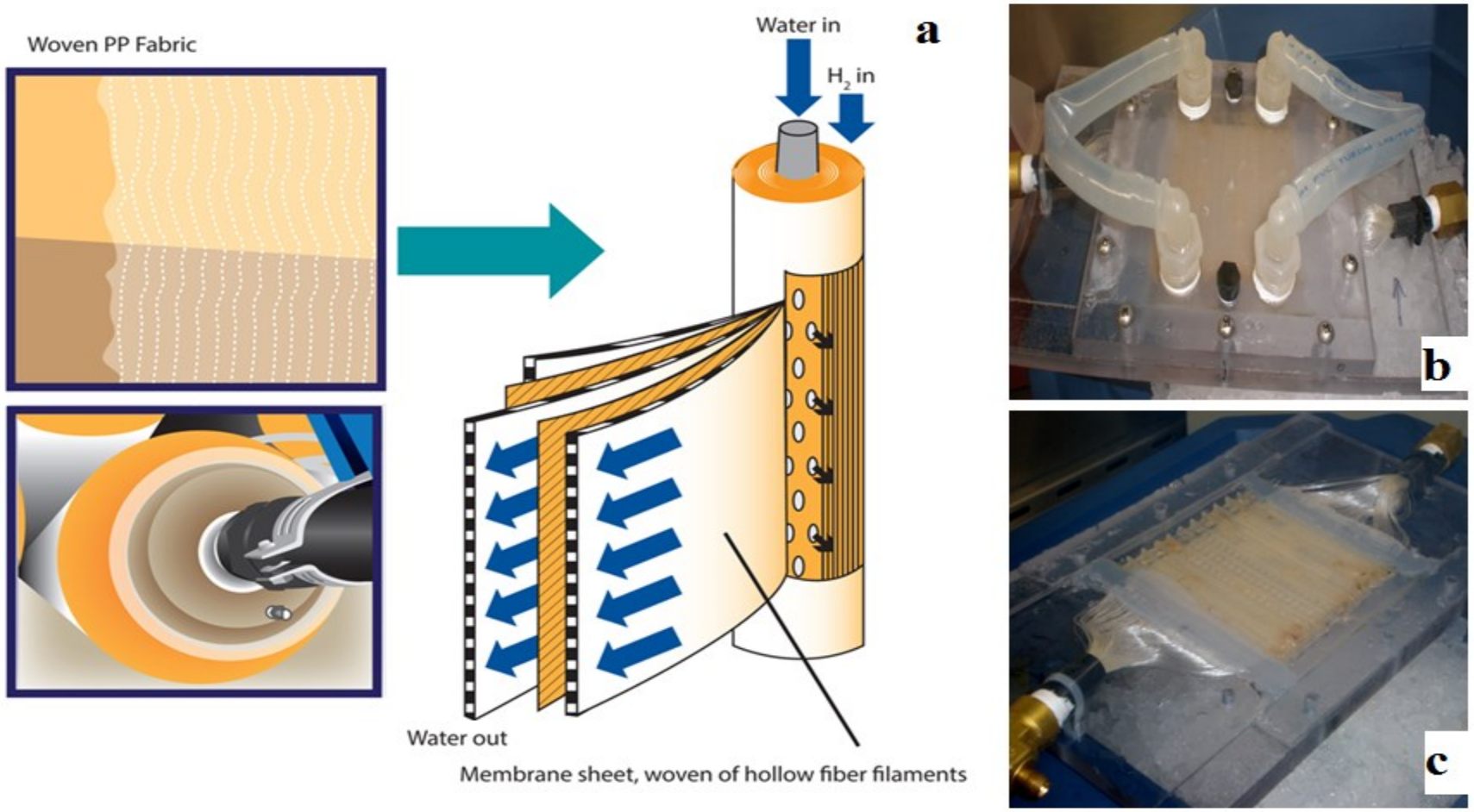

Figure 1 **a** Pilot MBfR module which shows the ABS core and woven fabric. The water and H_2 flows are pointed by arrows. **b&c** show side reactors which were sent to ASU for community analysis. The side reactors were operated as the pilot MBfRs. **b** shows the water lines feeding the side reactors, and **c** visualizes the gas connections for the H_2 fed, and a closer look of the biofilm in the fiber sheet.

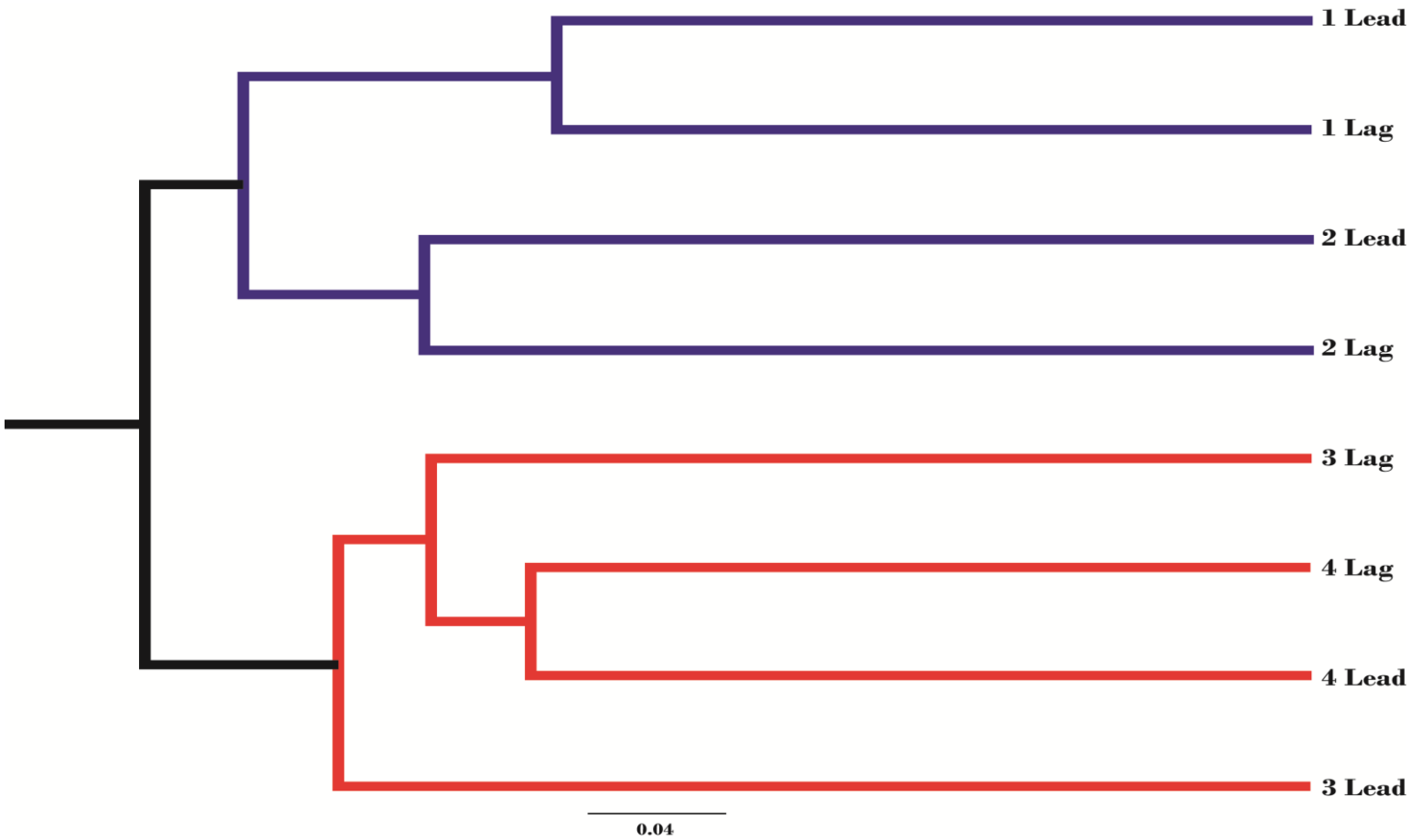

Figure 2 Clustering based on the unweighted UniFrac analyses. The branch length represents the distance between biofilm samples in UniFrac units, as indicated by the scale bar. The labels on each branch indicate the biofilm sample of either lead or lag MBfR at the four conditions applied to the reactors. The blue branch correspond to the reactors operated at high electron acceptor surface loadings (Conditions 1 and 2), while the red branch reflect the microbial community performing under low total electron acceptor surface loading (Conditions 3 and 4).

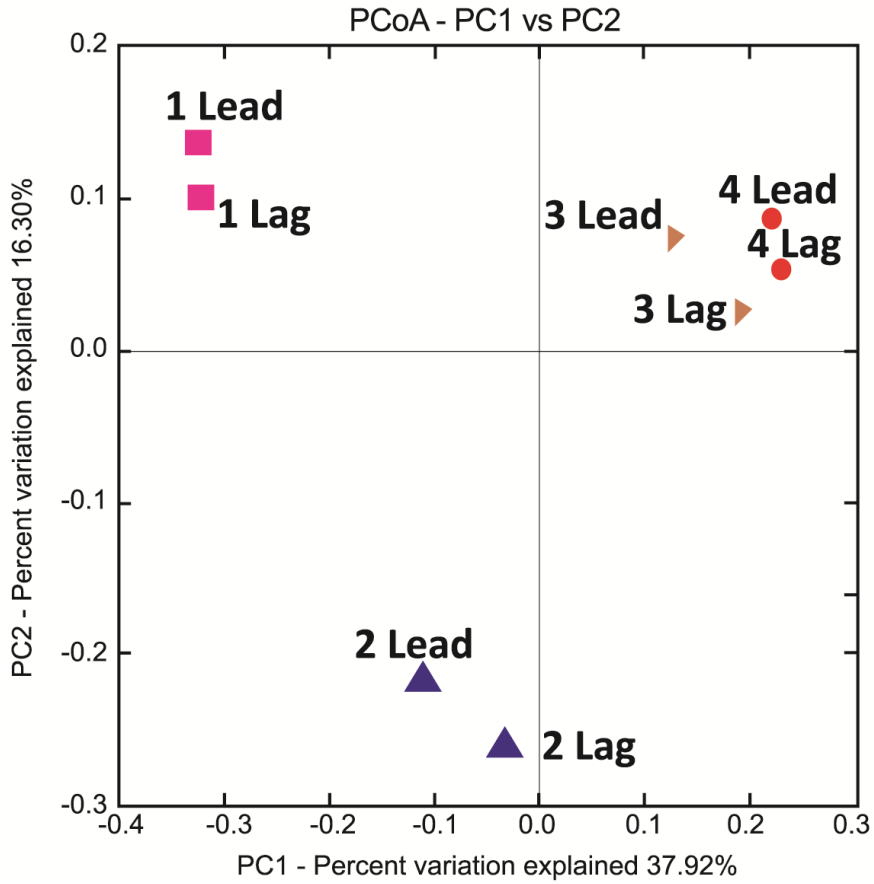

Figure 3 Principal Coordinate Analysis (PCoA) based on the unweighted UniFrac.

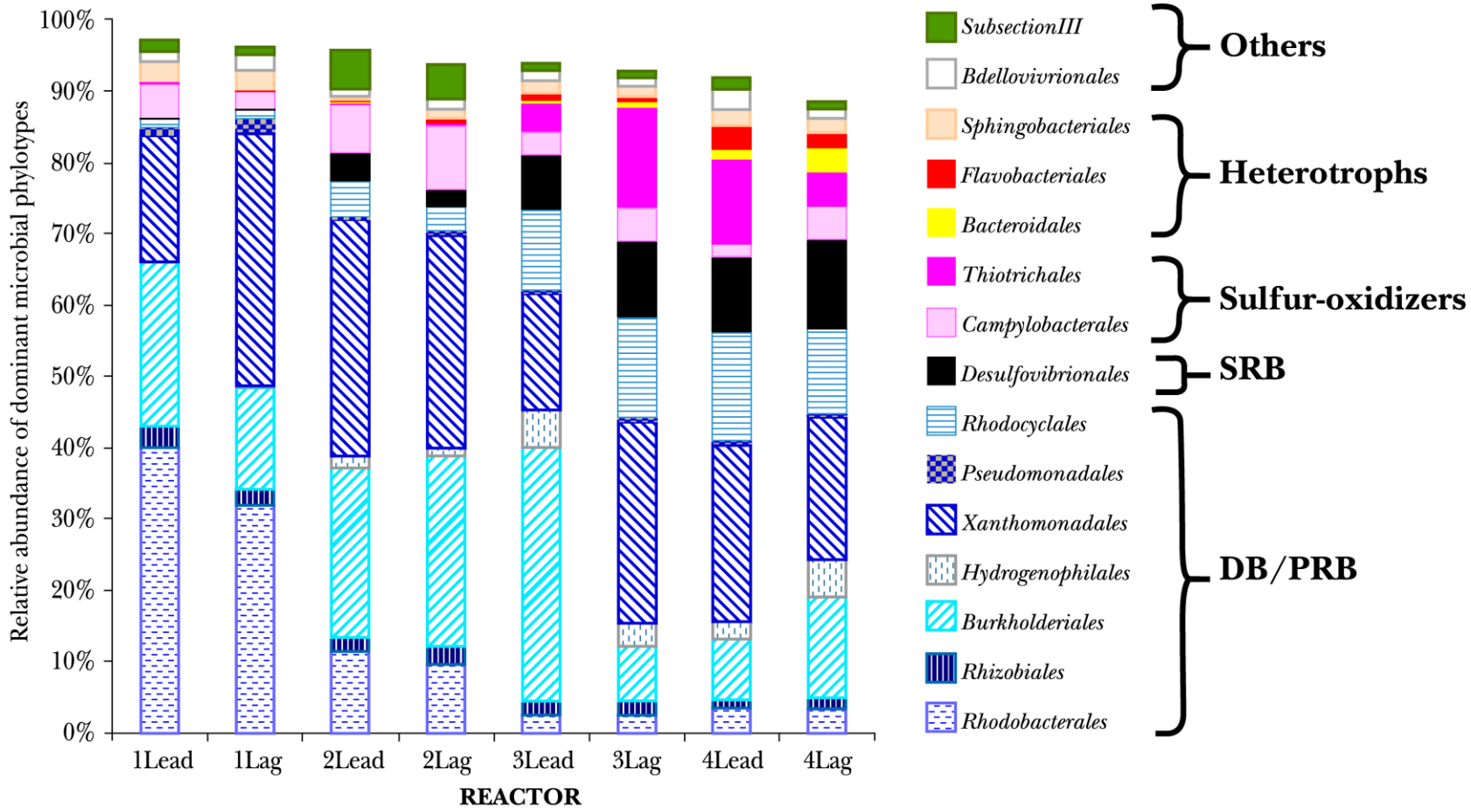

Figure 4 Microbial community structure in lead and lag MBfRs at the order level. The sum does not add up to 100% in all cases because phylotypes < 1% are not shown. The brackets in the legend group the orders according to known members of the noted metabolic groups. DB/PRB phylotypes are shown which hatched fills that clearly show a decline from Condition 1 to Condition 4. Some members of the "heterotrophic microorganisms," are capable of denitrification under specific circumnstances, such as when using acetate as electron donor and carbon source.[48]

References

(1) Knobeloch, L.; Salna, B.; Hogan, A.; Postle, J.; Anderson, H. Blue babies and nitrate-contaminated well water. *Environmental Health Perspectives*, **2000,** *108* (7): 675.

(2) Camargo, J. A.; Alonso, Á. Ecological and toxicological effects of inorganic nitrogen pollution in aquatic ecosystems: a global assessment. Environment international, **2006,** *32*(6): 831-849.

(3) US EPA. Basic Information about Nitrate in Drinking Water. http://water.epa.gov/drink/contaminants/basicinformation/nitrate.cfm (accessed February 17, 2014).

(4) US EPA. Perchlorate treatment technology update. No.EPA 542-R-05-015. **2005.**

(5) US EPA. Perchlorate. http://water.epa.gov/drink/contaminants/unregulated/perchlorate.cfm (accessed February 17, 2014).

(6) US EPA. Potential SBAR Panel: Drinking water regulatory actions for perchlorate. http://www.epa.gov/rfa/perchlorate.html (accessed January 30, 2014).

(7) Kim, K.; Logan, B. E. Fixed-Bed bioreactor treating perchlorate-contaminated waters. *Environ. Eng. Sci*. **2000,** *17* (5): 257-265.

(8) Lee, K. C.; Rittmann, B. E. Applying a novel autohydrogenotrophic hollow-fiber membrane biofilm reactor for denitrification of drinking water. *Water Res*. **2002,** *36*: 2040-2052.

(9) Zhang, H.; Bruns, M. A.; Logan, B. E. Perchlorate reduction by a novel chemolithoautotrophic, hydrogen-oxidizing bacterium. *Environ. Microbiol*. **2002,** *4* (10): 570–576.

(10) Hatzinger, P. B. Perchlorate biodegradation for water treatment. *Environ. Sci. Technol.* **2005,** *39* (11): 239A-247A.

(11) Herman, D. C.; Frankenberger, W. T. 1998. Microbial-mediated reduction of perchlorate in groundwater. *J Environ Qual,* **1998**, *27*(4): 750-754.

(12) Herman, D. C.; Frankenberger, W. T. Bacterial reduction of perchlorate and nitrate in water. *J Environ Qual*, **1999,** *28*(3): 1018-1024.

(13) Chaudhuri, S. K.; O'Connor, S. M.; Gustavson, R. L.; Achenbach, L. A.; Coates, J. D. Environmental factors that control microbial perchlorate reduction. *Appl Environ Microbiol*, **2002,** *68*(9): 4425-4430.

(14) Coates, J. D.; Achenbach, L. A. Microbial perchlorate reduction: rocket fuelled metabolism. *Nature Rev Microbiol* **2004,** *2*(7): 569-580.

(15) Tang, Y.; Zhao, H.-P.; Marcus, A. K.; Krajmalnik-Brown, R.; Rittmann, B. E. A steady-state biofilm model for simultaneous reduction of nitrate and perchlorate -- Part 2: Parameter optimization and results and discussion. *Environ Sci Technol* **2012,** *46*(3): 1608-1615.

(16) Romanenko, V. I.; Koren'kov, V. N.; Kuznetsov, S. I. Bacterial decomposition of ammonium perchlorate. *Mikrobiologiia*, **1976,** *45*(2): 204.

(17) Hochstein, L. I.; Tomlinson, G. A. The enzymes associated with denitrification. *Annu. Rev. Microbiol.* **1988,** *42*: 231– 261

(18) Kengen, S. W. M.; Rikken, G. B.; Hagen, W. R.; van Ginkel, C. G.; Stams, A. J. M. Purification and characterization of (per)-chlorate reductase from the chlorate-respiring strain GR-1 J. *Bacteriol*. **1999,** *181*: 6706– 6711

(19) Logan, B. E.; Wu, J.; Unz, R. F. Biological perchlorate reduction in high-salinity solutions. *Water Res*, **2001,** *35*(12): 3034-3038.

(20) Min, B.; Evans, P. J.; Chu, A. K.; Logan, B. E. Perchlorate removal in sand and plastic media bioreactors. *Water Res*, **2004,** *38*(1): 47-60.

(21) Evans, P.; Smith, J.; Singh, T.; Hyung, H.; Arucan, C.; Berokoff, D.; Friese, D.; Overstreet, R.; Vigo, R.; Rittmann, B. E.; Ontiveros-Valencia, A.; Zhao, H.-P.; Tang, Y.; Kim B.-O., van Ginkel, S.; Krajmalnik-Brown, R. Final Report: Nitrate and Perchlorate Destruction and Potable Water Production Using Membrane Biofilm Reduction. ESTCP Project ER-200541 **2013.**

(22) Rittmann, B. E. The membrane biofilm reactor is a versatile platform for water and wastewater treatment. *Environ. Eng. Res.* **2007,** *12* (4): 157-175.

(23) Zhao, H.-P.; Ontiveros-Valencia, A.; Tang, Y.; Kim, B.-O.; van Ginkel, S.; Friese, D.; Overstreet, R.; Smith, J.; Evans, P.; Krajmalnik-Brown, R.; Rittmann, B. E. Removal of multiple electron acceptors by pilot-scale, two-stage membrane biofilm reactors. *Water Res.* **2014**, *54*: 115-122.

(24) Ontiveros-Valencia, A.; Tang, Y.; Krajmalnik-Brown, R.; Rittmann, B. E. Perchlorate reduction from a highly contaminated groundwater in the presence of sulfate-reducing bacteria in a hydrogen-fed biofilm. *Biotechnol Bioeng* **2013,** *110*(12): 3139-3147.

(25) Ontiveros-Valencia, A.; Tang, Y; Krajmalnik-Brown, R.; Rittmann, B. E. Managing the interactions between sulfate- and perchlorate-reducing bacteria when using hydrogen-fed biofilms to treat a groundwater with a high perchlorate concentration. *Water Res.* **2014,** *55*: 215-224.

(26) Waller, S. Bioremediation of perchlorate-contaminated groundwater. Master thesis. University of Toronto. **2002.**

(27) Attaway, H.; Smith, M. Reduction of perchlorate by an anaerobic enrichment culture. *J Ind Microbiol* **1993,** *12*(6): 408-412.

(28) Bardiya, N.; Bae, J. H. Bioremediation potential of a perchlorate-enriched sewage sludge consortium. *Chemosphere* **2005,** *58*(1): 83-90.

(29) Lozupone, C.; Knight, R. UniFrac: a new phylogenetic method for comparing microbial communities. *App. Environ. Microbiol*. **2005,** *71*: 8228-8235.

(30) Lozupone, C.; Hamady, M.; Knight, R. UniFrac - an online tool for comparing microbial community diversity in a phylogenetic context. *BMC Bioinformatics* **2006,** *7*(1): 371.

(31) Tang, Y.; Zhou, C.; Van Ginkel, S.; Ontiveros-Valencia, A.; Shin, J.; Rittmann, B. E. Hydrogen-Permeation Coefficients of the Fibers Used in H_2-Based Membrane Biofilm Reactors. *J. Membrane Sci.* **2012,** *407-408*: 176-183.

(32) Sun, Y.; Wolcott, R. D.; Dowd, S. E. Tag-encoded FLX amplicon pyrosequencing for the elucidation of microbial and functional gene diversity in any environment. High-Throughput Next Generation Sequencing. *Meth. Mol. Biol*. **2011,** *733*: 129-141.

(33) Ontiveros-Valencia, A.; Ilhan, Z. E.; Kang, D.-W.; Rittmann, B. E.; Krajmalnik-Brown, R. Phylogenetic analysis of nitrate- and sulfate-reducing bacteria in a hydrogen-fed biofilm. *FEMS Microbiol. Ecol.* **2013,** *85*: 158-167.

(34) Caporaso, J. G.; Kuczynski, J.; Stombaugh, J.; Bittinger, K.; Bushman, F. D.; Costello, E. K.; Fierer, N.; Pena, A. G.; Goodrich, J. K.; Gordon, J. I.; Huttley, G. A.; Kelley, S. T.; Knight, D.; Koenig, J. E.; Ley, R. E.; Lozupone, C. A.; McDonald, D.; Muegge, B. D.; Pirrung, M.; Reeder, J.; Sevinsky, J. R.; Tumbaugh, P. J.; Walters, W. A.; Widmann, J.; Yatsunenko, T.; Zaneveld, J.; Knight, R. Qiime allows analysis of high-throughput community sequencing data. *Nat. Methods* **2010,** *7*: 335-336.

(35) Edgar, R. C. Search and clustering orders of magnitude faster than blast. *Bioinformatics* **2010,** *26*: 2460-2461.

(36) DeSantis, T. Z.; Hugenholtz, P.; Larsen, N.; Rojas, M.; Brodie, E. L.; Keller, K.; Huber, T.; Dalevi, D.; Hu, P.; Andersen, G. L. Greengenes, a chimera-checked 16s rrna gene database and workbench compatible with arb. *Appl. Environ. Microbiol.* **2006,** *72*: 5069-5072.

(37) Caporaso, J. G.; Bittinger, K.; Bushman, F. D.; DeSantis, T. Z.; Andersen, G. L.; Knight, R. Pynast: A flexible tool for aligning sequences to a template alignment. *Bioinformatics* **2010,** *26*: 266-267.

(38) Haas, B. J.; Gevers, D.; Earl, A. M.; Feldgarden, M.; Ward, D. V.; Giannoukos, G.; Ciulla, D.; Tabaa, D.; Highlander, S. K.; Sordergren, E.; Methé, B.; DeSantis, T. Z.; The Human Microbiome Consortium, Petrosino, J. F.; Knight, R.; Birren, B. W. Chimeric 16s rrna sequence formation and detection in sanger and 454-pyrosequenced pcr amplicons. *Genome Res.* **2011,** *21*: 494-504.

(39) Pruesse, E.; Quast, C.; Knittel, K.; Fuchs, B. M.; Ludwig, W.; Peplies, J.; Gloeckner, F. O. Silva. A comprehensive online resource for quality checked and aligned ribosomal RNA sequence data compatible with ARB. *Nucleic Acids Res.* **2007,** *35*: 7188-7196.

(40) Price, M. N.; Dehal, P. S.; Arkin, A. P. FastTree: computing large minimum evolution trees with profiles instead of a distance matrix. *Mol. Biol. Evol.* **2009,** *26*: 1641-1650.

(41) Hughes, J. B.; Hellmann, J. J.; Ricketts, T. H.; Bohannan, B. J. Counting the uncountable: statistical approaches to estimating microbial diversity. *Appl. Environ. Microbiol.* **2001,** *67* (10): 4399-4406.

(42) Faith, D. P. Conservation evaluation and phylogenetic diversity. *Biol. Conserv.* **1992,** *61*: 1-10.

(43) Shannon, C. E. A mathematical theory of communication. Bell System Technical Journal. **1948,** *27*: 379–423.

(44) Simpson, E. H. Measurement of diversity. *Nature* **1949,** *163*: 688.

(45) Ontiveros-Valencia, A.; Ziv-El, M.; Zhao, H.-P.; Feng, L.; Rittmann, B. E.; Krajmalnik-Brown, R. Interactions between nitrate-reducing and sulfate-reducing bacteria coexisting in a hydrogen-fed biofilm. *Environ. Sci. Technol.* **2012,** *46*: 11289-11298.

(46) Tang, Y.; Ontiveros-Valencia, A.; Liang, F.; Zhou, C.; Krajmalnik-Brown, R.; Rittmann, B. E. A biofilm model to understand the onset of sulfate reduction in denitrifying membrane biofilm reactors. *Biotechnol. Bioeng.* **2012,** *110*: 763-772.

(47) Wu, W.-M.; Gu, B.; Fields, M. W.; Gentile, M.; Ku, Y.-K.; Yan, H.; Tiquias, S.; Yan, T.; Nyman, J.; Zhou, J.; Jardine, P. M.; Craig, C. S. Uranium reduction by denitrifying biomass. *J. Bioremed*. **2005,** *9* (1): 41-61.
(48) Adav, S. S.; Lee, D. J.; Lai, J. Y. Microbial community of acetate utilizing denitrifiers in aerobic granules. Applied microbiology and biotechnology, **2010,** *85*(3), 753-762.
(49) Madigan, M.; Markinko, J.; Stahl, D.; Clark, D. Brock Biology of microorganisms; 12th ed.; Pearson: San Francisco California **2009.**
(50) Williams, T. M.; Unz, R. F. Isolation and characterization of filamentous bacteria present in bulking activated sludge. *Appl. Microbiol. Biotechnol.* **1985,** *22* (4): 273-282.
(51) Williams, T. M.; Unz, R. F.; Doman, J. T. Ultrastructure of Thiothrix spp. and "type 021N" bacteria. *Appl. Environ. Microbiol*. **1987,** *53* (7): 1560-1570.
(52) Zhao, H.-P.; Ilhan, Z. E.; Ontiveros-Valencia, A.; Tang, Y.; Rittmann, B. E.; Krajmalnik-Brown, R. Effects of multiple electron acceptors on microbial interactions in a hydrogen-based biofilm. *Environ. Sci. Technol.* **2013,** *47*: 7396-7403.
(53) Martin, K. J.; Picioreanu, C.; Nerenberg, R. Multidimensional modeling of biofilm development and fluid dynamics in a hydrogen-based, membrane biofilm reactor (MBfR). *Water Res.* **2013,** *47* (13): 4739-4751.
(54) Roldan, M. D. Chlorate and nitrate reduction in phototrophic bacteria Rhodobacter capsulatus and Rhodobacter sphaeroides. *Curr. Microbiol.* **1994,** *29*: 241-245